Catalysis Today 164 (2011) 2–8

Contents lists available at ScienceDirect

Catalysis Today

journal homepage: www.elsevier.com/locate/cattod

Value-added olefin-based materials originating from FI catalysis: Production of vinyl- and Al-terminated PEs, end-functionalized PEs, and PE/polyethylene glycol hybrid materials

Kaori Matoishi, Kazuoki Nakai, Naoshi Nagai, Hiroshi Terao, Terunori Fujita*

Mitsui Chemicals, Inc., 580-32 Nagaura, Sodegaura, Chiba 299-0265, Japan

ARTICLE INFO

Article history:
Received 29 June 2010
Received in revised form
24 November 2010
Accepted 27 November 2010
Available online 14 January 2011

Keywords:
FI catalysts
Vinyl-terminated PEs
Al-terminated PEs
End functionalized PEs
PE/PEG hybrid materials
Self assembly

ABSTRACT

This contribution reports on the selective synthesis of vinyl- and Al-terminated polyethylenes (PEs) using FI catalysts with dried methylaluminoxane (DMAO) or DMAO/trimethylaluminum, and the conversion of the resultant vinyl-terminated PEs to end-functionalized PEs and PE/polyethylene glycol (PEG) hybrid materials. The materials that are derived from the vinyl-terminated PEs are new PE-based materials featuring the presence of polar functional groups or polar polymer segments. Zr-FI catalysts containing sterically less encumbered substituents (e.g., methyl, cyclobutyl, cyclopentyl) on the imine-Ns selectively formed vinyl-terminated PEs (M_w 1900–14,000, vinyl functionality > 90%) with high efficiency. Conversely, a Zr-FI catalyst containing a sterically encumbered substituent (i.e., 2-*i*-propylphenyl) at the same position exclusively provided Al-terminated PEs (M_w 12,000–716,000) with high activity. Therefore, the selection of the particular substituent on the imine-N resulted in the selective production of both vinyl- and Al-terminated PEs. Starting from the vinyl-terminated PEs that were produced using the FI catalysts, epoxy-, diol-, triol-, diamino-, and succinic anhydride-terminated PEs and PE/PEG AB_2- and AB_3-type hybrid materials were developed with unique material properties.

1. Introduction

Historically, the development of high-activity molecular catalysts for olefin polymerization has been behind the creation of value-added polymers with new or enhanced material properties [1]. This is because highly active catalysts are capable of displaying substantial activities, even after the catalyst design (aiming at the creation of precisely controlled polymers) that normally diminishes the activity of the resulting catalyst. In short, highly active molecular catalysts generally possess a wide variety of catalyst design possibilities.

Notable examples of this historical development route include the development of highly active group 4 metallocene catalysts for the production of high performance polymers, including linear low-density PEs, amorphous ethylene/1-butene copolymers, ethylene/norbornene copolymers, ethylene/propylene/diene elastomers, and syndiotactic polypropylenes (PPs) and polystyrenes [2,3]. Many of these high performance polymers created with group 4 metallocene catalysts have been commercialized and have impacted our daily lives in countless beneficial ways.

Additionally, the development of high-activity molecular transition metal catalysts supported by heteroatom-based ligands (post-metallocene catalysts) has given rise to differentiated polymers that were unobtainable using conventional catalysts [e.g., hyper-branched PEs, ethylene/methyl acrylate copolymers, α-olefin-based block copolymers, highly isotactic PPs using solution polymerization conditions] [4–12].

In our own work, we have developed highly active molecular phenoxy–imine ligated early transition metal catalysts (a.k.a. FI catalysts) for the (co)polymerization of olefinic monomers, based on ligand-oriented catalyst design research [13]. FI catalysts, after activation, show a number of unique features, which include extremely high monomer selectivity (ethylene > α-olefins), highly isoselective and syndioselective enchainments of propylene and styrene monomers, high functional group tolerance, precise control over chain transfers, and MAO- and borate-free polymerization catalysis [14–16].

Because of the above features, FI catalysts have given rise to a wide variety of olefin-based materials [e.g., ultra-high molecular weight linear PEs, ethylene- and α-olefin-based block copolymers, ethylene- and/or propylene-based end-functionalized (co)polymers, regio- and stereoirregular high molecular weight poly(1-hexene)s, ultra-fine non-coherent PE particles], some of which are now beginning to enter the industrial phase [14].

* Corresponding author. Tel.: +81 438 64 2308; fax: +81 438 64 2490.
E-mail address: Terunori.Fujita@mitsui-chem.co.jp (T. Fujita).

0920-5861/$ – see front matter © 2011 Published by Elsevier B.V.
doi:10.1016/j.cattod.2010.11.078

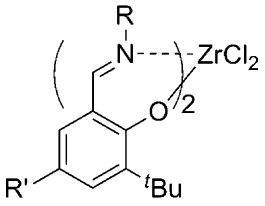

	R	R'		R	R'
1	methyl	H	**9**	cyclobutyl	H
2	ethyl	H	**10**	cyclobutyl	methyl
3	*n*-propyl	H	**11**	cyclopentyl	H
4	*i*-propyl	H	**12**	cyclohexyl	H
5	*t*-butyl	H	**13**	2-methylcyclohexyl	H
6	*n*-hexyl	H	**14**	phenyl	H
7	*n*-hexyl	methyl	**15**	2-methylphenyl	H
8	cyclopropyl	H	**16**	2-*i*-propylphenyl	H

Fig. 1. FI catalysts **1**–**16** employed in this study.

In this paper, we would like to discuss the selective synthesis of both vinyl- and Al-terminated PEs using Zr-FI catalysts [17,18]. Additionally, we will summarize the transformation of vinyl-terminated PEs into end-functionalized PEs and PE/polyethylene glycol (PEG) hybrid materials, which are new PE-based materials featuring the presence of polar functional groups or polar polymer segments [18–20]. The results introduced herein indicate the importance of the development of highly active catalysts for the creation of value-added olefin-based materials.

2. Selective vinyl- and Al-terminated PEs

The FI catalysts **1**–**16** that were employed in this study are shown in Fig. 1. FI catalysts **8**–**16** were prepared according to previously reported procedures [21]. Conversely, FI catalysts **1**–**7** were synthesized by the reaction of the lithium salts of the corresponding phenoxy–imine ligands with $ZrCl_4(thf)_2$ using a similar method.

FI catalysts **1**–**16** have a series of substituents on the imine-Ns; the substituents being in close proximity to the Cl-bound sites (polymerization sites after activation) when an FI catalyst has a six-coordinated metal center. X-ray crystallographic investigations demonstrated that FI catalysts **2**, **7**, **10**, **12**, and **14** possess six-coordinated metal centers in an approximately octahedral structure with a *trans*-O, *cis*-N, and *cis*-Cl arrangement (Fig. 2) [18,21]. We assume that other FI catalysts adopt similar structures.

The molecular structures shown in Fig. 2 reveal that the substituents on the imine-Ns, which are located on a plane at the backside of the Cl-bound sites, are in fact the nearest groups to the Cl-bound sites (except for FI catalyst **10,** in which the substituent *ortho* to the phenoxy-O is the nearest group to the Cl-bound site), suggesting that the substituent on the imine-N is the strategic substituent vis-à-vis catalyst design [14]. The distances between the Cl atom and its nearest C atom in the substituent on the imine-N are 3.80 Å (**2**), 4.00 Å (**7**), 4.96 Å (**10**), 4.19 Å (**12**), and 3.79 Å (**14**). Conversely, the distances between the Cl atom and its nearest C atom in the substituent *ortho* to the phenoxy-O (*t*-butyl group) are 4.00 Å (**2**), 4.12 Å (**7**), 4.13 Å (**10**), 4.23 Å (**12**), and 4.12 Å (**14**). These considerable differences in steric environments near the active sites may affect the polymerization catalysis of these FI catalysts.

The results of ethylene polymerization (0.1 MPa, 25 °C) using FI catalysts **1**–**16** with dried MAO (DMAO) activation (Al/Zr ratio: 6250) are compiled in Table 1. Most of the FI catalysts investigated were highly active toward ethylene polymerization (displaying much higher activities than Cp_2ZrCl_2/DMAO: 28 kg-PE/mmol-cat/h) and formed PEs having relatively low molecular weights (M_w 1900–174,000) [18]. A general trend was observed in that the introduction of a sterically bulkier substituent on the imine-N usually resulted in increased molecular weight of the product. Namely, some correlation between the product molecular weight and the steric bulk of the substituent on the imine-N was observed for a series of FI catalysts [i.e., methyl (R–H 33 Å^3) M_w 2600, ethyl (52 Å^3) M_w 5300, *n*-propyl (70 Å^3) M_w 9100, *i*-propyl (70 Å^3) M_w 14,700; cyclobutyl (79 Å^3) M_w 1900, cyclopentyl (95 Å^3) M_w 3800, cyclohexyl (111 Å^3) M_w 13,800, methylcyclohexyl (129 Å^3) M_w 162,000; and phenyl (99 Å^3) M_w 7100, methylphenyl (117 Å^3) M_w 174,000; the volume of R–H was calculated using the Spartan '02 software package from Wavefunction, Inc.].

The enhanced product molecular weight mediated by the sterically bulkier substituent presumably suggests that the chain transfer(s) involved is (are) more sensitive to steric congestion than ethylene insertion because molecular weight is determined by the relative rate of chain propagation and chain termination.

It is interesting to note that an acyclic alkyl group (smaller than ~100 Å^3 in volume) on the imine-N normally provides a higher molecular weight PE relative to a cycloalkyl group on the basis of the steric bulk of the substituent (Fig. 3), though the molecular weight seems to reach a plateau value in the case of the acyclic alkyl groups. We postulate that an acyclic alkyl group with a small carbon number behaves as a sterically larger substituent than a cycloalkyl group having the same carbon number because of its higher degree of freedom. The higher degree of freedom may provide larger steric congestion near the active site. An acyclic alkyl group with a large carbon number, however, gives similar steric congestion near the active site though the volume of the group is larger, resulting in the observation of a plateau molecular weight value. For the cycloalkyl groups investigated (FI catalysts **8**–**13**), a larger cycloalkyl group gives a higher molecular weight PE because of the increased steric congestion near the active site.

It can be seen from Fig. 4 that the steric bulk of the substituent on the imine-N, and in particular, steric congestion near the active sites, plays a decisive role in determining the chain-end

Table 1
Ethylene polymerization using FI catalysts **1**–**16** with DMAO.

Entry	FI catalyst	Yield (g)	Activity[a]	M_w[b]/10^3	M_w/M_n[b]	Vinyl end[c] (%)
1	**1**	1.06	64	2.6	1.8	96
2	**2**	0.66	40	5.3	1.9	89
3	**3**	0.91	55	9.1	1.9	84
4	**4**	2.03	122	14.7	1.9	54
5	**5**	Trace	–[d]	–[d]	–[d]	–[d]
6	**6**	1.09	65	9.7	1.8	80
7	**7**	0.84	53	10.1	1.9	79
8	**8**	0.64	38	4.8	1.8	91
9	**9**	0.56	34	1.9	1.6	92
10	**10**	0.43	26	1.9	1.6	91
11	**11**	1.94	116	3.8	1.8	91
12	**12**	3.41	204	13.8	1.8	90
13	**13**	2.54	152	162	3.9	52
14	**14**	4.35	261	7.1	2.0	88
15	**15**	0.69	41	174	2.2	18
16	**16**	1.24	74	125	2.1	0

Conditions: solvent, toluene (250 mL); polymerization temperature, 25 °C; FI catalyst 0.2 μmol, DMAO 1.25 mmol, ethylene feed 100 L/h; polymerization time, 5 min.
[a] kg-PE/mmol-cat/h.
[b] Determined with GPC using PE calibration.
[c] Determined by ^{1}H NMR.
[d] Not determined.

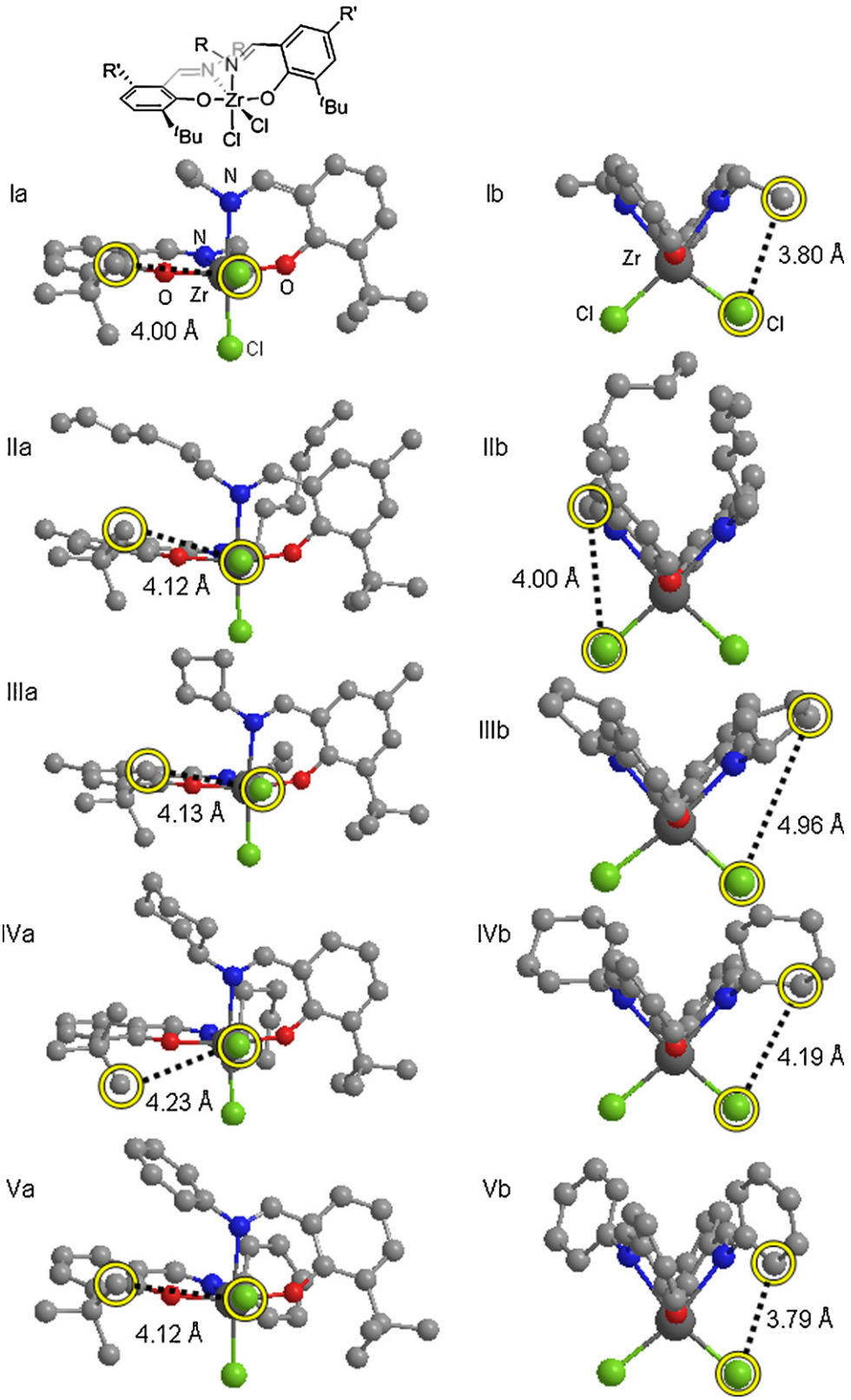

Fig. 2. Molecular structures of FI catalysts **2** (I), **7** (II), **10** (III), **12** (IV), and **14** (V). Hydrogen atoms are omitted for clarity. Ib–Vb display the structures viewed in a perpendicular direction to the N–Zr–Cl plane (*t*-butyl groups are omitted).

structures of the resulting PEs. FI catalysts **1**, **8**–**12** with sterically less encumbered substituents such as methyl, cyclobutyl and cyclopentyl groups generated PEs with predominant vinyl chain-ends (>90%) (vinyl-terminated PEs). These FI catalysts are the first examples of group 4 metal-based catalysts that produce well-defined vinyl-terminated PEs with high efficiency at ambient temperature [18].

The formation of vinyl-terminated PEs suggests that the main chain transfer of these FI catalysts is a β-H transfer. Further studies proved that the molecular weights were apparently independent

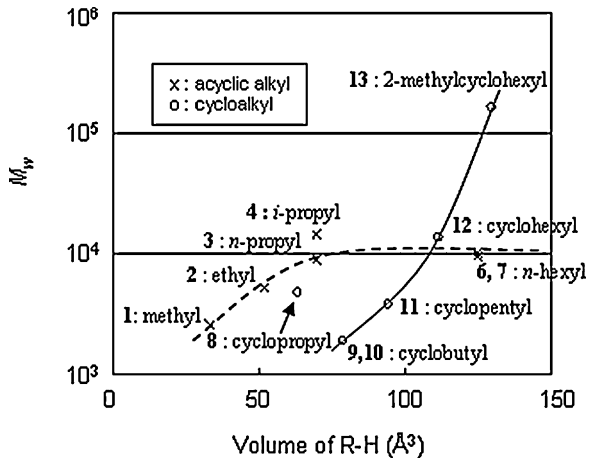

Fig. 3. Plots of product molecular weight as a function of the calculated R–H volume of the substituent on the imine-N (Table 1, entries 1–4, and 6–13).

of ethylene concentration, whereas the activities enhanced linearly with increasing ethylene concentration, showing that both chain propagation and β-H transfer are first order with respect to ethylene concentration. Based on these results, together with DFT calculations (which revealed the extremely unstable nature of the Zr–H species that is formed in the β-H transfer to the Zr metal), we concluded that the β-H transfer involved in these polymerizations is the β-H transfer to the incoming monomer (not to the Zr metal) [18].

The β-H transfer to the incoming monomer (which is a bimolecular β-H transfer) requires the Zr–C–C–H unit (presumably having β-agostic interaction) and the incoming ethylene to assume a roughly coplanar conformation, which probably results in a more encumbered six-centered transition state than the compact four-centered transition state for the chain propagation (ethylene insertion) or the unimolecular β-H transfer to the Zr metal. Since the substituents on the imine-Ns are in close proximity to the active sites, the substituents may undergo direct interactions with an intermediate and a transition state for the β-H transfer to the incoming monomer.

It should be noted that the presence of a cycloalkyl group on the imine-N generally yields a PE with a higher degree of vinyl unsaturation compared with an acyclic alkyl group, on the basis of the steric bulk of the substituent (Fig. 4). We infer that the reason for this observation is that the cycloalkyl group provides a sterically

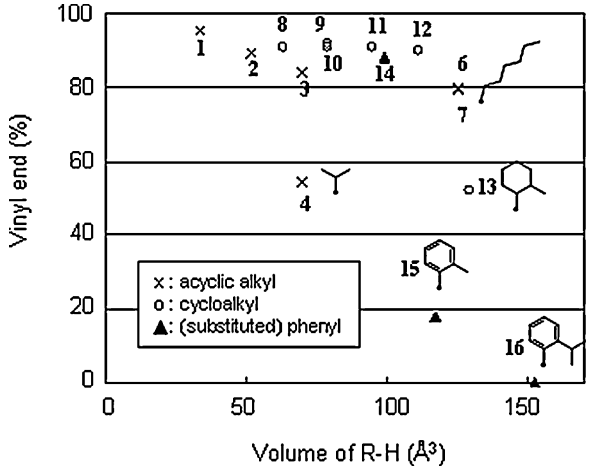

Fig. 4. Plots of vinyl selectivity as a function of the calculated R–H volume of the substituent on the imine-N (Table 1, entries 1–4, and 6–16).

Table 2
Ethylene polymerization using FI catalyst **16** with DMAO or DMAO/Me_3Al.

Entry	Me_3Al[a] (mmol)	Al/Zr molar ratio	Yield (g)	Activity[b]	M_w[c]/10^3	M_w/M_n[c]
1	0	500	2.41	58	716	2.6
2	0.200	900	2.48	60	36.8	2.0
3	0.375	1250	2.09	50	28.3	2.2
4	1.000	2500	1.88	45	18.6	2.0
5	2.250	5000	1.63	39	13.3	2.1
6	3.500	7500	1.42	34	11.9	2.0
7	6.000	12,500	1.07	26	10.2	2.1

Conditions: solvent, toluene (250 mL); polymerization temperature, 25 °C; FI catalyst 0.5 μmol, DMAO 0.250 mmol, ethylene feed 100 L/h; polymerization time, 5 min.
[a] Amount of trimethylaluminium.
[b] kg-PE/mmol-cat/h.
[c] Determined with GPC using PE calibration.

less-encumbered environment to the active sites, relative to the corresponding acyclic alkyl group.

Although, generally speaking, FI catalysts favor β-H transfer to the incoming monomer (Table 1, Fig. 4), a significant increase in the steric congestion near the active site (i.e., *i*-propyl, 2-methylcyclohexyl, 2-methyphenyl and 2-*i*-propylphenyl groups) mitigates the β-H transfer and another route for terminating the chain growth in the form of a chain transfer to an alkylaluminum becomes more prominent.

FI catalyst **16,** which possesses a 2-*i*-propylphenyl group on the imine-N, with MAO activation (Al/Zr ratio: 500) exclusively produced PE having an alkylaluminum chain-end (Al-terminated PE), which changed to a saturated chain-end during a work-up process [17]. The exclusive formation of the Al-terminated PE was confirmed by the ^{13}C NMR study of the PE obtained with deuterolytic workup. Due to the marked preference for the chain transfer to an alkylaluminum group in MAO and/or trimethylaluminum, well-defined Al-terminated PEs having low-to-very-high molecular weights (M_w 10,200–716,000, M_w/M_n 2.0–2.6) were synthesized quantitatively by FI catalyst **16** combined with DMAO or DMAO/trimethylaluminum (Al/Zr ratio: 500–12,500) (Table 2).

Therefore, the selection of the substituent on the imine-N (the substituent being located at a strategic place vis-à-vis polymerization catalysis) resulted in the selective synthesis of both vinyl- and Al-terminated PEs with high productivity.

The well-defined vinyl- and Al-terminated PEs that are formed using FI catalysts possess reactive chain-ends, and thus they may serve as reactive PEs or distinctive intermediates. For instance, the vinyl-terminated PEs can serve as well-defined macromonomers in copolymerization reactions with ethylene or α-olefin to form long-chain branched polymers. Additionally, the vinyl- and Al-terminated PEs may function as new building blocks in the production of end-functionalized PEs, and PE- and polar polymer-based block or graft copolymers (PE/polar polymer hybrid materials) [22–27].

3. End-functionalized PEs

Although some established methods for the conversion of an Al-terminated PE to an end-functionalized PE are available (conversion to –OH, –Cl, –Br, –I, etc.), little is known about effective methods for the transformation of a vinyl-terminated PE into an end-functionalized PE by chain-end functionalization [28,29]. We believe that vinyl-terminated PEs are more useful materials than Al-terminated PEs due to their higher versatility vis-à-vis functionalization, in addition to their ease of handling. We therefore aimed at developing useful methods for converting vinyl-terminated PEs to end-functionalized PEs with high efficiency.

Initial attempts to prepare end-functionalized PEs were unsuccessful because of the relatively low reactivity of a vinyl C=C bond compared with an Al–C bond toward functionalization, and this

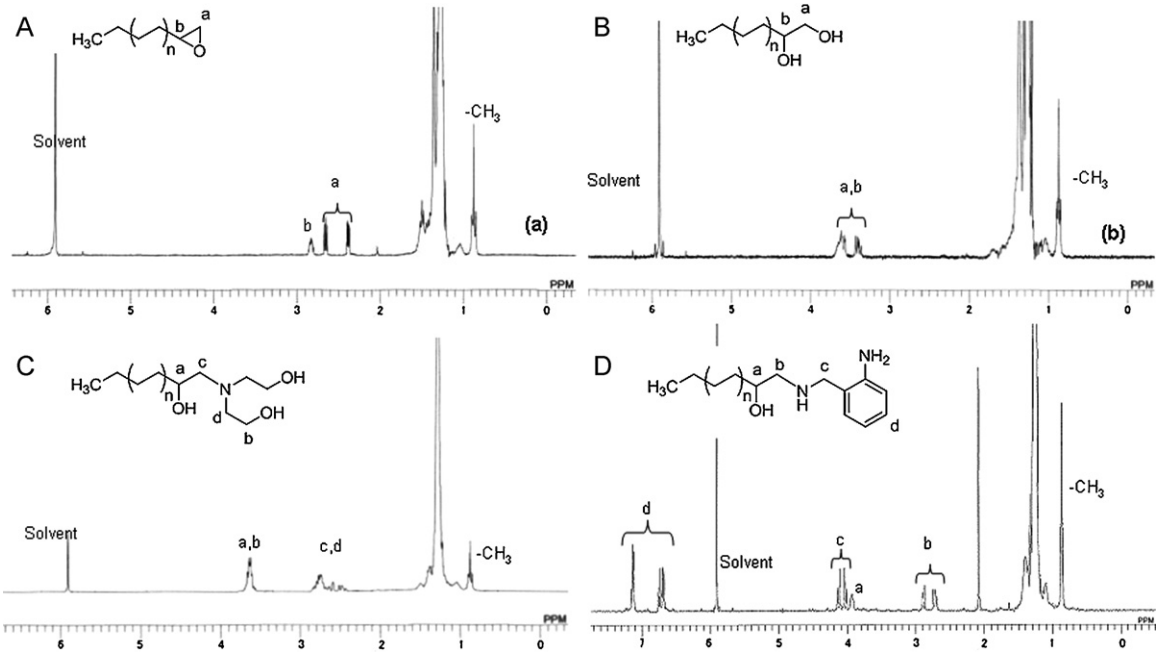

Fig. 5. ^{1}H NMR spectra of epoxy-, diol-, triol-, and dianimo-terminated PE.

normally resulted in the low conversion of a vinyl-terminated PE and/or the predominant formation of isomerized products of a vinyl-terminated PE. To our delight, however, we found that vinyl-terminated PEs are easily transformed to epoxy-terminated PEs with hydrogen peroxide oxidation using a toluene/water biphasic system in the presence of a phase transfer agent [18]. For example, the treatment of a vinyl-terminated PE (M_w 2000, M_w/M_n 2.4, vinyl functionality 95%, T_m 122 °C) with hydrogen peroxide (30% water solution) in toluene using Na_2WO_4 as a catalyst and methyl-tri-*n*-octylammonium hydrogen sulfate at 90 °C afforded the corresponding epoxy-terminated PE (M_w 2000, M_w/M_n 1.8, epoxy functionality 96%, T_m 121 °C) in practically quantitative yield (Fig. 5).

The development of the above method, which converts a vinyl-terminated PE to an epoxy-terminated PE in virtually quantitative yield, has opened up a new dimension in the field of end-functionalized PE synthesis (Fig. 6). Namely, epoxy-terminated PEs worked as intermediates for a wide variety of functionalized PEs due to their high reactivity toward a nucleophile. For example, the *in situ* hydrolysis of the epoxy-terminated PE above (M_w 2000, M_w/M_n 1.8, epoxy functionality 96%, T_m 121 °C) using aqueous 2-propanol quantitatively yielded the corresponding diol-terminated PE (M_w 2000, M_w/M_n 1.8, diol functionality 95%, T_m 121 °C). In addition, the epoxy-terminated PE reacted with diethanolamine at 140 °C to give the corresponding triol-terminated PE (M_w 2000, M_w/M_n 1.8, triol functionality 94%, T_m 121 °C). Furthermore, the reaction of the epoxy-terminated PE (M_w 1400, M_w/M_n 2.0, vinyl group 95%, T_m 116 °C) with 2-aminomethylaniline at 150 °C provided the corresponding diamino-terminated PE (M_w 1700, M_w/M_n 2.0, diamino functionality 95%, T_m 120 °C).

Conversely, the Alder-Ene reaction of a vinyl-terminated PE (M_w 1400, M_w/M_n 2.0, vinyl group 95%, T_m 116 °C) with maleic anhydride in the presence of 2,6-di-*t*-butyl-4-methylphenol as a radical quencher at 195 °C furnished the corresponding succinic anhydride-terminated PE (M_w 1700, M_w/M_n 1.7, succinic anhydride functionality 102%, T_m 117 °C) (Fig. 7(A)). The succinic anhydride-terminated PE exhibited higher thermal stability than its parent vinyl-terminated PE due to the presence of the chain-end succinic anhydride group, though the above introduced epoxy-, diol-, triol-, and diamino-terminated PEs displayed thermal stabilities similar to their parent vinyl-terminated PEs [19].

Interestingly, the corresponding disodium succinate-terminated PE existed as nano-sized particles (diameter 10–30 nm) and worm-like fibers (fiber diameter 20–30 nm, length 60–270 nm) in a 1 wt% water dispersion, which was prepared at 120–130 °C (above the T_m of the PE segment) under pressurized conditions (Fig. 7(B)) The nano-sized particles and fibers are probably formed through the self-assembly of the hydrophobic PE chains as cores and the self-assembly of the chain-end hydrophilic [$Na_2(COO)_2R$] segments at the particle surfaces that insulate the PE segments from water.

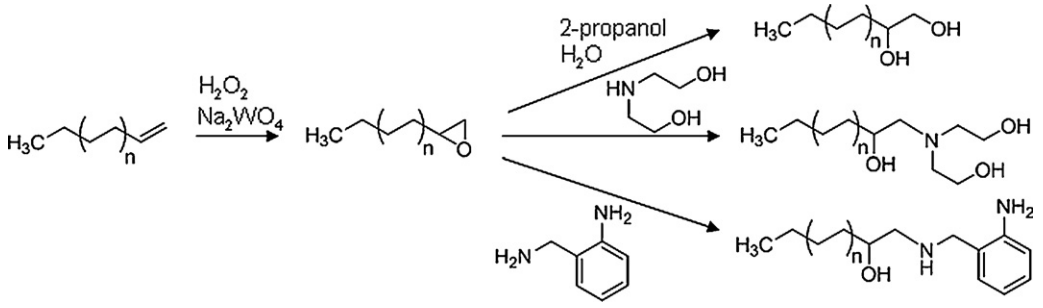

Fig. 6. Synthesis of end-functionalized PEs from vinyl-terminated PE.

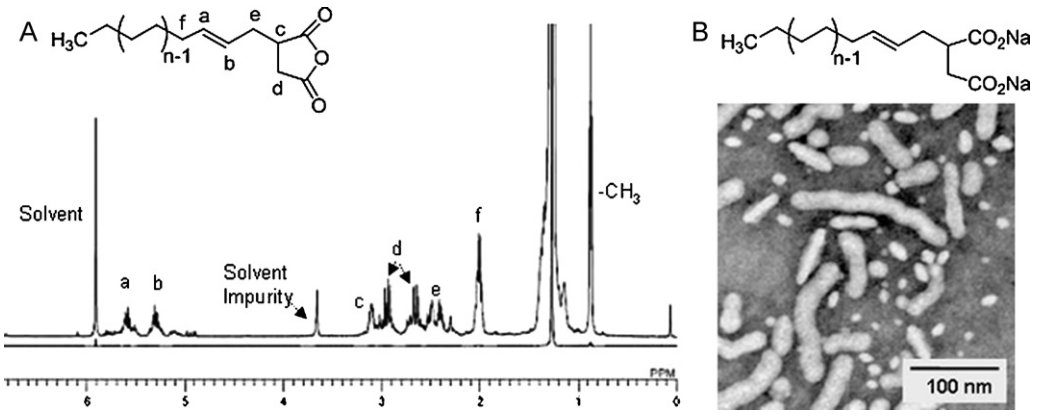

Fig. 7. ^{1}H NMR spectrum of succinic anhydride-terminated PE (A) and TEM image of the nano-sized particles and worm-like fibers composed of disodium succinate-terminated PE (1 wt% water dispersion) (B).

The end-functionalized PEs introduced herein possess unique features that combine the properties of PE (e.g., T_m and melting enthalpy) and reactive polar functional groups, and thus should have many potential applications across a broad range of fields (e.g., bi- or tri-functional monomers, cationic surfactants, heat-resistant waxes and additives, film-surface modifiers, anti-wear agents for inks and coatings), depending on the functional groups that were introduced to the parent PEs.

4. PE/polyethylene glycol (PEG) hybrid materials

The well-defined and highly reactive end-functionalized PEs described above served as precursors for a wide array of PE/polar polymer hybrid materials (linear and branched hydrophobic/hydrophilic polymers) that are comprised of PE and polyester, polyurethane or polyethylene glycol (PEG) segments. Among these amphiphilic materials, PE/PEG hybrid materials, and in particular PE/PEG AB_3-type hybrid materials, displayed characteristic features [20].

Treatment of the triol-terminated PE (M_n 1100, M_w/M_n 1.8, triol functionality 94%, T_m 121 °C) with ethylene oxide using KOH as a catalyst led to the formation of PE/PEG AB_3-type hybrid materials [AB_3 hybrid materials, PE: M_n 1100, PEG: M_n 1200 (average M_n 400 × 3), T_m 120 °C]. Likewise, the corresponding AB_2-type hybrid materials [AB_2 hybrid materials, PE: M_n 1100, PEG: M_n 1200 (average M_n 600 × 2), T_m 120 °C] were synthesized by the reaction of the a diol-terminated PE (M_n 1100, M_w/M_n 1.8, diol functionality 95%, T_m 121 °C) and ethylene oxide. Therefore, two structurally different PE/PEG hybrid materials having the same PE/PEG composition were successfully obtained. The AB_3 and AB_2 hybrid materials were characterized by ^{1}H and ^{13}C NMR, FT-IR, DSC, and GPC.

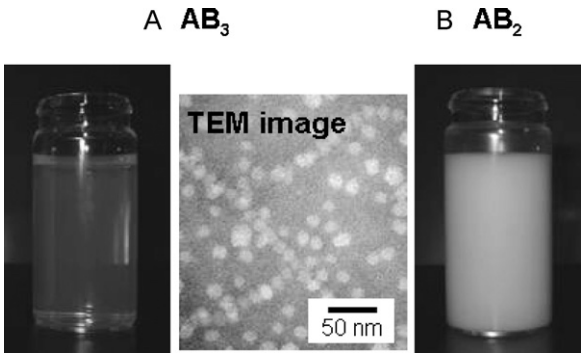

Fig. 8. Water dispersions of AB_3 (A) and AB_2 (B) hybrid materials (5 wt%).

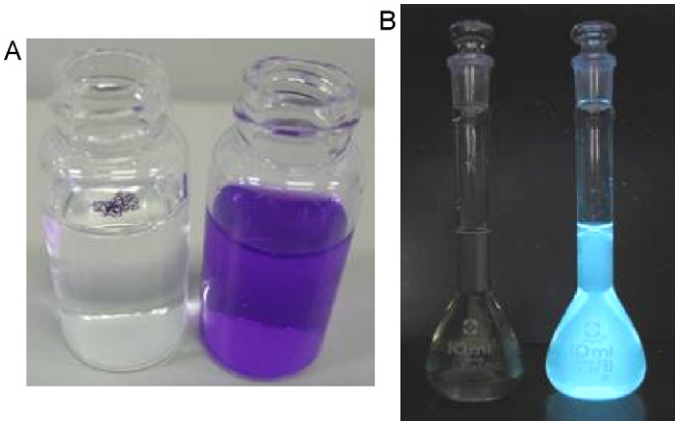

Fig. 9. 2,7,12,17-tetra-*t*-Butyl-5,10,15,20-tetraazaporphyrinato copper (II) (0.07 mmol) or 8-anilino-1-naphthalene sulfonic acid (0.01 mmol) with water (10 mL) in the absence [A (left), B (left)] or in the presence of AB_3 nanoparticles [0.2 wt%; A (right), B (right)].

Surprisingly, the AB_3 hybrid materials can form nano-sized particles in water, unlike conventional functionalized polyolefins. Fig. 8(A) displays a picture of a 5 wt% water dispersion of the AB_3 hybrid materials, which was prepared at 130 °C under pressurized conditions. As can be seen, the water dispersion appears semi-transparent, containing nano-sized particles with an average particle size of 18 nm [TEM image, Fig. 8(A)], which is in sharp contrast to the water dispersion of the corresponding AB_2 hybrid materials (Fig. 8(B), where the average particle size was 2 μm, and for dispersions of conventional maleic anhydride-grafted polyolefins, where the average particle size was 2–10 μm). Therefore, the AB_2 and AB_3 hybrid materials showed significantly different aggregation behavior in water, which resulted in stable dispersions consisting of particles of remarkably different sizes.[1]

The AB_3-type molecular architecture obviously accounts for the unprecedented behavior described above. The difference in the behavior in water between the AB_3 and AB_2 hybrid materials clearly indicates that the polymer structure (AB_3 and AB_2) rather than the polymer composition (PE/PEG ratio) predominantly determines the behavior of the PE/PEG hybrid materials in this case.

As anticipated, these nano-sized particles exhibited a number of unique features. For instance, they are able to include 2, 7, 12, 17-

[1] AB_2 hybrid materials can form nano-sized particles in water as a result of elaborate material design [e.g., PE: M_n 1100, PEG: M_n 2200 (average M_n 1100 × 2), average particle size 20 nm].

tetra-*t*-butyl-5,10,15,20-tetraazaporphyrinato copper (II) (a water insoluble dye) inside the particles in water, resulting in the formation of a purple-colored water dispersion (Fig. 9(A)). Moreover, the nano-sized particles can accept 8-anilino-1-naphthalene sulfonic acid (which is an environmentally sensitive fluorescent probe that does not produce fluorescence in water under UV light irradiation), yielding fluorescence under UV light irradiation in water (Fig. 9(B)). These results suggest that the three hydrophilic-PEG-segments of the AB_3 hybrid materials effectively insulate the PE segments from water, making the inside of the nano-sized particles a highly hydrophobic environment.

5. Conclusion

In the introduction, we described how, historically, the development of high activity olefin polymerization catalysts has been behind the creation of value-added polymers. We discovered highly active phenoxy–imine ligated early transition metal complexes (a.k.a. FI catalysts) for olefin polymerization. As expected, FI catalysts possess a wide range of catalyst design possibilities, and elaborate catalyst design focusing on the substituents on the imine-Ns led to the development of unique FI catalysts, which are capable of selectively producing well-defined vinyl- and Al-terminated PEs with high efficiency.

Using the vinyl-terminated PEs formed with the FI catalysts, we have successfully created end-functionalized PEs and PE/PEG AB_2 and AB_3 hybrid materials. These unique PE-based materials featuring the presence of a polar functional group or a polar polymer segment possess distinctive macromolecular architectures and associated properties, and thus they may serve as valuable materials in numerous fields.

It was the development of high activity FI catalysts that made it possible to selectively produce vinyl-terminated PEs with high productivity, which in turn gave rise to the creation of well-defined end-functionalized PEs and PE/PEG hybrid materials. The results introduced in this paper underline the great importance of the development of high activity olefin polymerization catalysts (FI catalysts) for the creation of value-added olefin-based materials.

Appendix A. Notes

A.1. Ethylene polymerization using FI catalysts with DMAO

To a well stirred solution of ethylene in toluene (250 ml) with a flow of ethylene gas (100 l/h) at 25 °C, a toluene solution of DMAO or DMAO/trimethylaluminum and then a toluene solution of an FI catalyst were added. After 5 min, 3 ml of *i*-butyl alcohol was added to terminate the polymerization. The resulting mixture was added to 1000 ml of acidified methanol (containing 2 ml of concentrated HCl). The resulting PE product was collected by filtration, washed with methanol, and dried *in vacuo* at 80 °C for 10 h.

A.2. Polymer characterization

^1H and ^{13}C NMR spectra for the produced PEs, end-functionalized PEs, and PE/PEG AB_2 and AB_3 hybrid materials were recorded on a JEOL JNM-EX270 spectrometer (270 MHz, ^1H NMR) and on a JEOL JNM-ECX400 spectrometer (100 MHz, ^{13}C NMR). The molecular weights (M_w and M_n) and the molecular weight distributions (M_w/M_n) were determined using a Waters GPC2000 gel permeation chromatograph equipped with four TSKgel columns (two sets of TSKgel GMH_6-HT, two sets of TSKgel GMH_6-HTL) at 140 °C using PE calibration. *o*-Dichlorobenzene was employed as a solvent at a flow rate of 1.0 ml/min.

References

[1] H. Makio, N. Kashiwa, T. Fujita, Adv. Synth. Catal. 344 (2002) 477–493.
[2] H.H. Brintzinger, D. Fischer, R. Mülhaut, B. Rieger, R.M. Waymouth, Angew. Chem., Int. Ed. Engl. 34 (1995) 1143–1170.
[3] A.L. McKnight, R.M. Waymouth, Chem. Rev. 98 (1998) 2587–2598.
[4] G.J.P. Britovsek, V.C. Gibson, D.F. Wass, Angew. Chem., Int. Ed. 38 (1999) 428–447.
[5] S.D. Ittel, L.K. Johnson, M. Brookhart, Chem. Rev. 100 (2000) 1169–1204.
[6] V.C. Gibson, S.K. Spitzmesser, Chem. Rev. 103 (2003) 283–316.
[7] Z. Cai, T. Shiono, J. Synth. Org. Chem. Jpn. 66 (2008) 664–672.
[8] D.W. Stephan, Organometallics 24 (2005) 2548–2560.
[9] P.D. Bolton, P. Mountford, Adv. Synth. Catal. 347 (2005) 355–366.
[10] W. Wang, T. Tanaka, M. Tsubota, M. Fujiki, S. Yamanaka, K. Nomura, Adv. Synth. Catal. 347 (2005) 433–446.
[11] P.M. Zeimentz, S. Arndt, B.R. Elvidge, J. Okuda, Chem. Rev. 106 (2006) 2404–2433.
[12] P.S. Chum, K.W. Swogger, Prog. Polym. Sci. 33 (2008) 797–819.
[13] T. Matsugi, T. Fujita, Chem. Soc. Rev. 37 (2008) 1264–1277.
[14] H. Makio, T. Fujita, Acc. Chem. Res. 42 (2009) 1532–1544.
[15] M. Mitani, J. Saito, S. Ishii, Y. Nakayama, H. Makio, N. Matsukawa, S. Matsui, J. Mohri, R. Furuyama, H. Terao, H. Bando, H. Tanaka, T. Fujita, Chem. Rec. 4 (2004) 137–158.
[16] Y. Nakayama, J. Saito, H. Bando, T. Fujita, Chem. Eur. J. 12 (2006) 7546–7556.
[17] J. Saito, Y. Tohi, N. Matsukawa, M. Mitani, T. Fujita, Macromolecules 38 (2005) 4955–4957.
[18] H. Terao, S. Ishii, J. Saito, S. Matsuura, M. Mitani, N. Nagai, H. Tanaka, T. Fujita, Macromolecules 39 (2006) 8584–8593.
[19] A.V.S. Sainath, M. Isokawa, M. Suzuki, S. Ishii, S. Matsuura, N. Nagai, T. Fujita, Macromolecules 42 (2009) 4356–4358.
[20] K. Matoishi, S. Nakatsuka, K. Nakai, M. Isokawa, N. Nagai, T. Fujita, Chem. Lett. 39 (2010) 1028–1029.
[21] S. Matsui, M. Mitani, J. Saito, Y. Tohi, H. Makio, N. Matsukawa, Y. Takagi, K. Tsuru, M. Nitabaru, T. Nakano, H. Tanaka, N. Kashiwa, T. Fujita, J. Am. Chem. Soc. 123 (2001) 6847–6856.
[22] T.C. Chung, Prog. Polym. Sci. 27 (2002) 39–85.
[23] J.-Y. Dong, Y. Hu, Coord. Chem. Rev. 250 (2006) 47–65.
[24] Y. Inoue, T. Matsugi, N. Kashiwa, K. Matyjaszewski, Macromolecules 37 (2004) 3651–3658.
[25] H. Kaneyoshi, K. Matyjaszewski, J. Appl. Polym. Sci. 105 (2007) 3–13.
[26] Y. Schneider, N.A. Lynd, E.J. Kramer, G.C. Bazan, Macromolecules 42 (2009) 8763–8768.
[27] W.-J. Wang, P. Liu, B.-G. Li, S. Zhu, J. Polym. Sci. Part A: Polym. Chem. 48 (2010) 3024–3032.
[28] T. Shiono, K. Soga, Macromol. Rapid Commun. 13 (1992) 371–376.
[29] H. Hagihara, T. Shiono, T. Ikeda, Macromolecules 30 (1997) 4783–4785.